Fusogenic Reactive Oxygen Species Triggered Charge-Reversal Vector for Effective Gene Delivery

*Xin Liu, Jiajia Xiang, Dingcheng Zhu, Liming Jiang, Zhuxian Zhou, Jianbin Tang, Xiangrui Liu, Yongzhuo Huang, and Youqing Shen**

Gene therapy has been proven to be an effective approach for cancer treatment with few side effects.[1] Nonviral gene vectors including cationic lipids, polymers, dendrimers and peptides are particularly attractive in terms of safety, low immunogenicity, biocompatibility, and the potential for large-scale manufacture.[2] However, their applications are bottlenecked by low transfection efficiency compared with viral vectors. Great efforts have therefore been devoted to increasing the gene transfection efficiency of nonviral vectors by screening molecular structures via combinatorial chemistry[3] and designing virus-mimicking nanostructures[4] or formulations[5] based on extensive mechanism studies[6] and improved tumor targeting.[7]

In nonviral gene delivery, cationic polymers are generally used to neutralize the negative charges of DNA and condense the large macromolecules into nanoparticles to protect them from degradation and facilitate its cellular internalization. However, DNA/polymer complexes (polyplexes) are thermodynamically stable and inherently resistant to dissociation, which is necessary to release the DNA for transcription once inside the cell.[8] Therefore, many designs have been proposed to facilitate DNA release including making polymers degradable into short chains and/or by exploiting pH-, reduction-, enzyme-, or temperature-mediated release mechanisms,[9] or lowering charge density.[10] However, it was shown that even a lipid molecule carrying a single cationic charge may interact with the DNA transcription machine and subsequently affect transcription,[8] let alone short cationic chains.

We propose a positive to negative charge-reversal concept in which the cationic polymer responds to intracellular signals and becomes fully negatively charged to quickly release the packed DNA, minimizing interference with the DNA transcription machine. Herein we demonstrate this concept using a reactive oxygen species (ROS)-labile charge-reversal polymer, poly[(2-acryloyl)ethyl(*p*-boronic acid benzyl)diethylammonium bromide] (B-PDEAEA). Upon oxidation of the boronic acid group by ROS (e.g., H_2O_2), the quaternary ammonium releases *p*-quinone methide (*p*-hydroxylmethylenephenol (HMP))[11] and becomes a tertiary amine, which subsequently self-catalyzes fast hydrolysis of the ester group producing poly(acrylic acid)[12] (**Scheme 1**a). Intracellular signaling ROS including H_2O_2, superoxide anions (O_2^-) and hydroxyl radicals are known to be elevated in cancerous cells[13] and capable of oxidizing benzylboronic acid/esters[13b,14] to trigger drug release,[14a] activation of prodrugs,[13b] and fluorescence.[15] Furthermore, boronic acid can form cyclic boronate esters with various diols and thus may be used to enhance the interaction of nanocarriers with cancer cells[16] or ribonucleotides of DNA and RNAs in gene delivery.[17] Importantly, boronate acid/esters and their end products are considered nontoxic to humans.[17b,18]

The general cellular internalization pathway of polyplex nanoparticles is endocytosis, which is mostly further trafficked into lysosomes, causing DNA degradation. A lipid envelope was thus further coated to the highly positive polyplexes and tuned to be able to fuse with cell membrane like a paramyxovirus[19] ejecting the polyplex into the cytosol, thereby avoiding the lysosome trapping (Scheme 1b). The virus-mimicking fusogenic lipopolyplexes (FLPPs) were very stable in blood circulation, effectively accumulated in the tumor, and efficiently expressed the carried genes after further PEGylated and functionalized with the tumor-homing short peptide CRGDK.

The synthesis of B-PDEAEA is shown in Scheme S1 (Supporting Information). The tertiary amine-based polymer poly[2-(*N*,*N*-diethylamino)ethyl acrylate] (PDEAEA) was prepared by radical polymerization. Its quaternization reaction with an excess of 4-(bromomethyl)phenylboronic acid produced water-soluble B-PDEAEA. The polymer effectively condensed plasmid DNA at *N*/*P* ratios of above 3, as probed by gel electrophoresis (Figure S1a, Supporting Information) and formed spherical polyplexes of ≈40 nm in diameter with a zeta potential of +15 to +20 mV (**Figure 1**a and Figure S1b, Supporting Information).

The premise of this design is ROS-triggered cascade charge reversal. The oxidation of the carbon–boron bond by H_2O_2 induced deboronation, followed by the release of *p*-quinone methide, which in water quickly turns into *p*-hydroxymethylphenol (HMP) (Scheme 1a). Thus, the ROS-responsiveness was tracked by the release of the intermediate HMP using high performance liquid chromatography (HPLC) (Figure 1b) and also NMR spectra (Figure S2, Supporting Information). In 1×10^{-3} M H_2O_2 the polymer degraded quickly in the first 30 min and almost completely within 2 h (Figure 1c). The charge reversal was monitored by the zeta potential change of

X. Liu, J. Xiang, D. Zhu, Dr. Z. Zhou, Prof. J. Tang, Prof. X. Liu, Prof. Y. Shen
Center for Bionanoengineering and Key Laboratory of Biomass Chemical Engineering of Ministry of Education
College of Chemical and Biological Engineering
Zhejiang University
Hangzhou 310027, China
E-mail: shenyq@zju.edu.cn
X. Liu, Prof. L. Jiang
Department of Polymer Science and Engineering
Zhejiang University
Hangzhou 310027, China
Prof. Y. Huang
Shanghai Institute of Materia Medica
Chinese Academy of Sciences
Shanghai 201203, China

DOI: 10.1002/adma.201504288

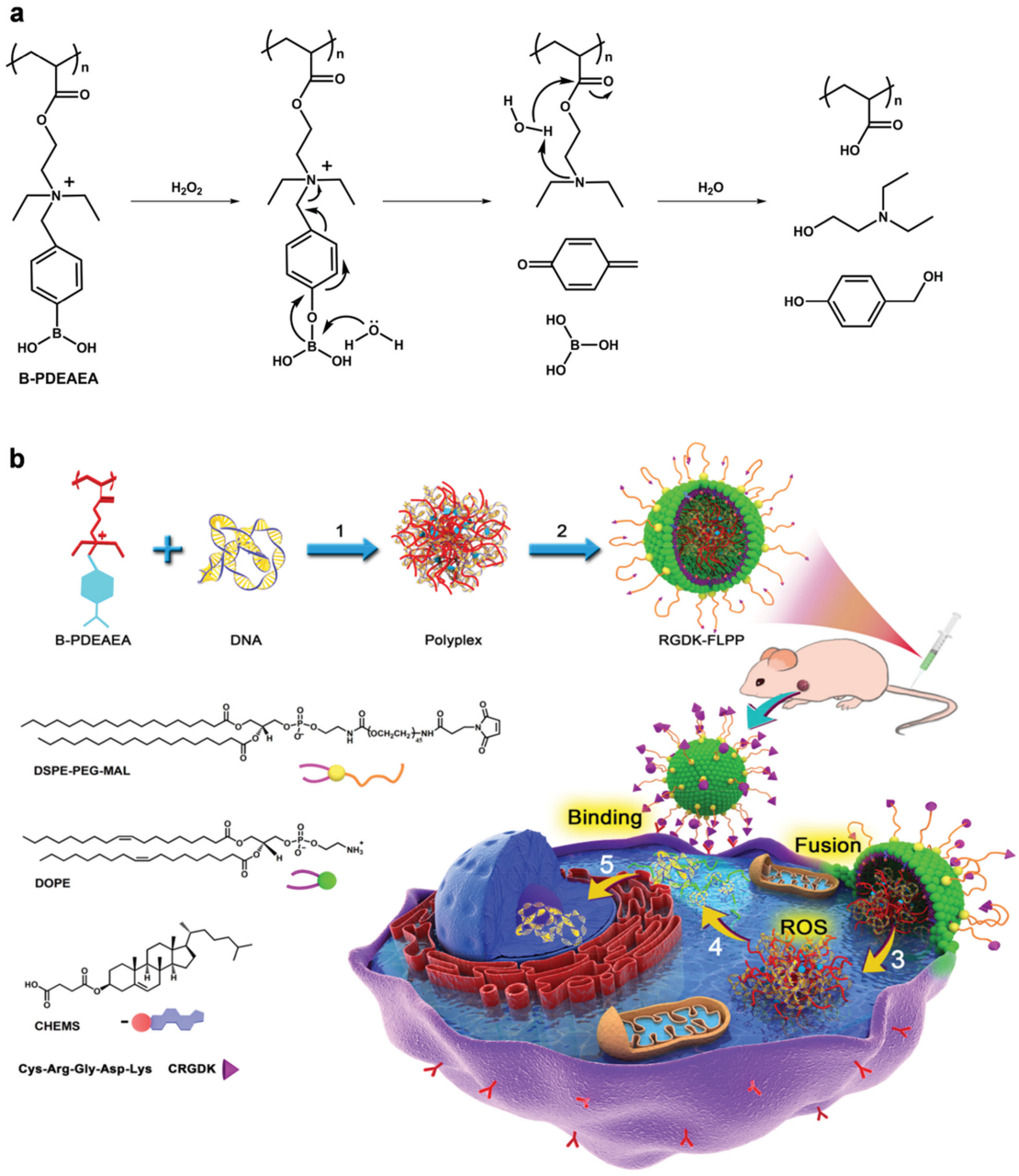

Scheme 1. Schematic representation of reaction oxygen species (ROS)-responsive charge-reversal polymer and its CRGDK-receptor targeting fusogenic lipopolyplex (RGDK-FLPPs) for systemic gene delivery. a) Poly2-acryloylethyl(*p*-boronic acid)benzyldiethylammonium bromide] (B-PDEAEA) and its ROS-triggered charge reversal to anionic polyacrylic acid; b) B-PDEAEA/DNA complexation forming polyplexes (1) and coating with lipids to form targeted FLPPs (2); Once intravenously injected, the FLPPs accumulate in tumor, where their RGDK ligands bind their receptors on the cell membrane, inducing the lipid layer to fuse with the cell membrane, ejecting the polyplexes into the cytosol (3); The intracellular ROS oxidize B-PDEAEA and trigger its charge reversal and release of DNA (4); The released DNA enters the nucleus for transcription (5).

B-PDEAEA in 4-(2-hydroxyethyl)-1-piperazineethanesulfonic acid (HEPES) buffer with H_2O_2. At pH 7.4, the zeta potential of B-PDEAEA quickly decreased from +28 to +17 mV, as the quaternary ammonium turned into a tertiary amine triggered by H_2O_2. Then the zeta potential decreased gradually as the ester group underwent self-catalyzed hydrolysis and produced poly(acrylic acid). The zeta potential became negative in ≈10 h. The charge-reversal was much faster, in less than 6 h, if B-PDEAEA was first incubated at pH 5.0 with H_2O_2 for 2 h and then at pH 7.4 because the oxidation potential of H_2O_2 is higher in acidic solution (Figure 1d). This suggests that if B-PDEAEA localizes in lysosomes for a while and then escapes, its charge-reversal would be accelerated. Accordingly, its polyplexes released the DNA after 1 h in 0.5×10^{-3} M H_2O_2 as detected by gel electrophoresis (Figure 1e). The loosening of the polyplexes was also reflected by their increased size, from 40 nm to

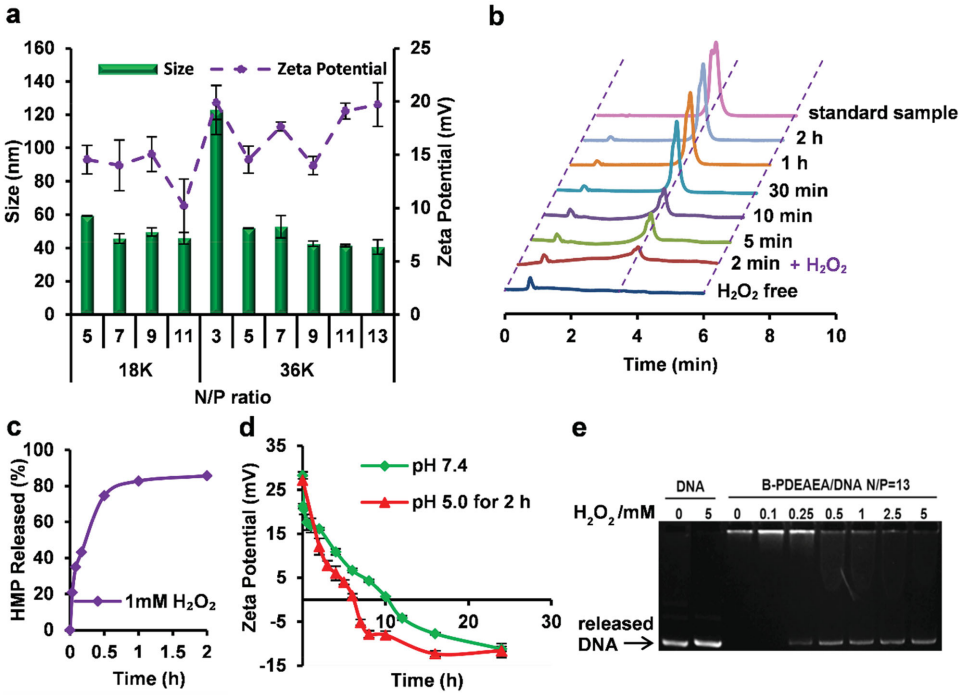

Figure 1. The DNA complexation and oxidative response of B-PDEAEA. a) The volume-averaged size and zeta potential of polyplexes of DNA with B-PDEAEA with different molecular weights at different *N*/*P* molar ratios. b) The HPLC traces of HMP released in the solution of 0.3 mg mL^{-1} B-PDEAEA with 1×10^{-3} M H_2O_2 at different times at 37 °C and c) the calculated release kinetics. d) The charge-reversal kinetics of B-PDEAEA (3 mg mL^{-1}) at 37 °C in pH 7.4 buffer with H_2O_2 or first incubated at pH 5.0 solution with H_2O_2 for 2 h and then at pH 7.4. The H_2O_2 concentration was 80×10^{-3} M. e) Gel retardation assay of DNA released from polyplexes at an *N*/*P* ratio of 13 after 1 h incubation in H_2O_2 solution at different concentrations at 37 °C.

≈1 μm (Figure S3, Supporting Information). The polymer had very low toxicity due to its conversion from a highly cationic state to polyacrylic acid, which has low toxicity (Figure S4, Supporting Information). Thus, the ROS-triggered charge-reversal vectors may be advantageous over rapidly biodegradable vectors (e.g., acid-cleavable vectors and bioreducible vectors) in that the resulting negatively charged polymer not only quickly releases DNA but also, unlike the degraded cationic fragments, does not interfere with the gene transcription process.

The overall in vitro gene transfection efficiency of B-PDEAEA polyplexes was evaluated using a luciferase plasmid as the reporter gene in A549, Hela, and SW480 cancer cells (**Figure 2**a and Figure S5, Supporting Information). In the serum-free medium, the highest luciferase transfection efficiency of B-PDEAEA polyplexes was achieved at an *N*/*P* ratio of 13, at which the transfection efficiency was 15 400 times higher than that of PDEAEA quaternized with iodomethane, (poly(*N*,*N*,*N*-diehylmethylaminoethyl acrylate, DEM), which is known to tightly pack DNA and have low intracellular dissociation and thus inefficient endosomal escape,[20] suggesting that the ROS-triggered charge reversal did play an important role in gene transfection. This transfection efficiency was also eight times higher than that of the gold standard, branched poly(ethylenimine) with a molecular weight of 25 KDa (PEI) at an *N*/*P* ratio of 7. Notably, the B-PDEAEA polyplexes at *N*/*P* ratios greater than 60 were not sensitive to serum any more, whose transfection efficiency was only slightly lower than the maximum transfection without serum and ≈100 times higher than that of PEI25K polyplexes under the same conditions (Figure 2a).

To further investigate whether intracellular ROS are involved in gene transfection of the B-PDEAEA polyplexes, diphenyleneiodonium (DPI), an inhibitor of intracellular ROS production mediated by flavoenzymes, particularly nicotinamide adenine dinucleotide phosphate (NAD(P)H) oxidase, was used to lower the intracellular ROS level.[21] As shown in Figure 2b, the luciferase gene expression in the DPI-treated cells decreased by up to two orders of magnitude, indicating that without ROS the polyplexes could not release the plasmids efficiently.

The efficiency of the polyplexes was further evaluated by measuring the percentage of cells expressing green fluorescence protein (GFP) using an enhanced green fluorescence protein (EGFP) reporter gene (Figure 2c,d). In the serum-free medium, B-PDEAEA polyplexes at an *N*/*P* ratio of 13 transfected 78.4% cells and the PEI polyplexes transfected 30.7% cells. In the medium with 10% serum, the B-PDEAEA polyplexes at an *N*/*P* ratio of 13 were no longer efficient and the PEI polyplexes could only transfected 5.0% of the cells; however, the B-PDEAEA polyplexes at high *N*/*P* ratios could still transfected 90.0% cells (Figure 2d). These results were clearly seen in the fluorescence microscopy that in the presence of serum PEI polyplexes transfected few cells, whereas the B-PDEAEA polyplexes transfected cells more and uniformly. To achieve high therapeutic efficacy in cancer gene therapy, it is more desirable for all of the cells to express an amount of therapeutic protein (e.g., tumor necrosis factor-related apoptosis-inducing ligand (TRAIL)) sufficient to induce apoptosis than for a few cells to express a large amount of the protein. Thus, compared with PEI-mediated gene transfection, B-PDEAEA is advantageous

ADVANCED MATERIALS
www.advmat.de

www.MaterialsViews.com

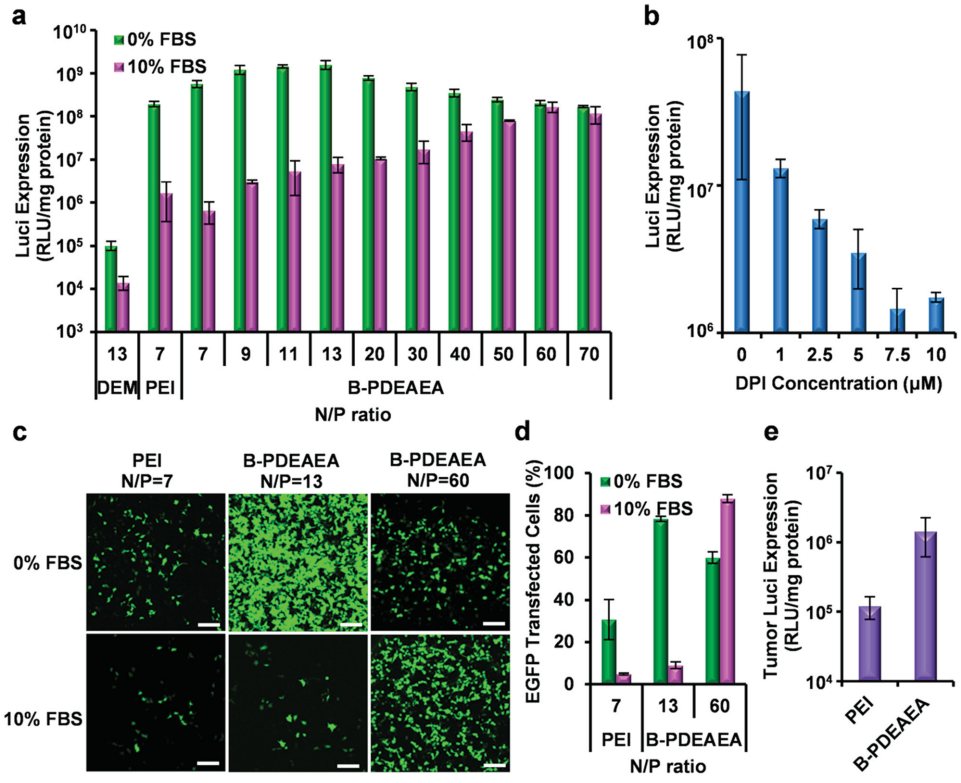

Figure 2. Gene transfection of polyplexes in A549 cells: a) Luciferase gene transfection of polyplexes without or with serum. Cells were transfected at 2.2 μg mL^{-1} DNA for 4 h followed by 44 h culture; the control polyplexes were of PEI ($N/P = 7$) or PDEAEA quaternized with iodomethane (DEM, $N/P = 13$). b) Luciferase expression of B-PDEAEA polyplexes in cells pretreated with ROS inhibitor DPI without serum. Cells were pretreated with DPI at different concentrations for 30 min and transfected at 2.2 μg mL^{-1} DNA for 4 h followed by 6 h culture with the same DPI concentration. c) EGFP gene transfection of PEI or B-PDEAEA polyplexes observed by fluorescence microscopy (scale bar = 200 μm); A549 cells (2.5×10^5) were transfected at 3.3 μg mL^{-1} DNA without or with 10% fetal calf serum (FBS) for 4 h followed by incubation in cell culture medium for 44 h, and d) EGFP transfection efficiency in terms of percentage of GFP-positive cells measured by flow cytometry. e) The A549-tumor luciferase transfection in nude mice at 48 h postintratumoral injection of polyplexes of B-PDEAEA ($N/P = 13$) or PEI ($N/P = 7$) ($n = 6$, 15 μg DNA per mouse in 60 μL HEPES).

in effectively infecting cells and inducing efficient gene expression in a list of commonly used tumor cells (Figures S5 and S6, Supporting Information).

The tumor gene transfection efficiency of B-PDEAEA and PEI polyplexes was examined after intratumoral injection. The luciferase expression in the tumor at 48 h postinjection of B-PDEAEA polyplexes with an N/P ratio of 13 was ≈12 times higher than the positive control PEI polyplexes (Figure 2e), indicating that the B-PDEAEA polyplexes would efficiently transfect tumor cells once arriving tumor tissue. Surprisingly, even though the in vitro transfection level of the polyplexes at an N/P ratio of 60 was higher in the presence of serum, their intratumoral transfection was lower than the polyplexes at an N/P ratio of 13 probably due to the hindered tumor penetration caused by the excess cationic polymer.

The intracellular trafficking of the B-PDEAEA polyplex in A549 cells was investigated to probe the mechanism behind its high transfection efficacy. Flow cytometry showed that cellular uptake of the polyplexes was suppressed at 4 °C, or by the inhibitor chlorpromazine, but not by filipin III, wortmannin, or cytochalasin D (**Figure 3**a); accordingly, the presence of chlorpromazine dramatically decreased the transfection efficiency (Figure 3b), indicating that its endocytosis was via the clathrin-mediated pathway. As observed by confocal microscopy (Figure 3c) and a movie in the Supporting Information, the polyplexes of Cy5-labeled DNA (red) with B-PDEAEA (N/P ratio of 13) first interacted with the cellular membrane and were internalized within only 5 min, probably due to the binding of the positively charged polyplexes to the negatively charged cell membrane and boronic acid to the glycocalyx.[22] Red fluorescence was initially associated with lysosomes stained by LysoTracker Green as yellow dots, but at 10 and 30 min, little red fluorescence was found in the lysosomes (Figure 3c and Figure S7, Supporting Information). Particularly, at 30 min most of the DNA did not overlap with the lysosomes but was scattered in the cytoplasm and some had even reached the nuclei (Figure 3c), indicating a quick and efficient escape of the polyplexes from the lysosomes. After 5 h incubation, more red fluorescence was visible in the perinuclear region and more red dots were visible in the nuclei (Figure 3c and see Figure S8 (Supporting Information) for enlarged view of full images). The ability of B-PDEAEA to escape from lysosomes was confirmed by a hemolysis assay.[23] The polymer induced 57% hemolysis at 20 μg mL^{-1} at pH 6.0 and almost 100% hemolysis at 40 μg mL^{-1} at pH 5.0 after 1 h incubation at 37 °C (Figure S9, Supporting Information).

The intracellular polyplex dissociation was observed by confocal microscopy using dually labeled polyplexes made from Cy5-labeled DNA (^{Cy5}DNA) and fluorescein isothiocyanate

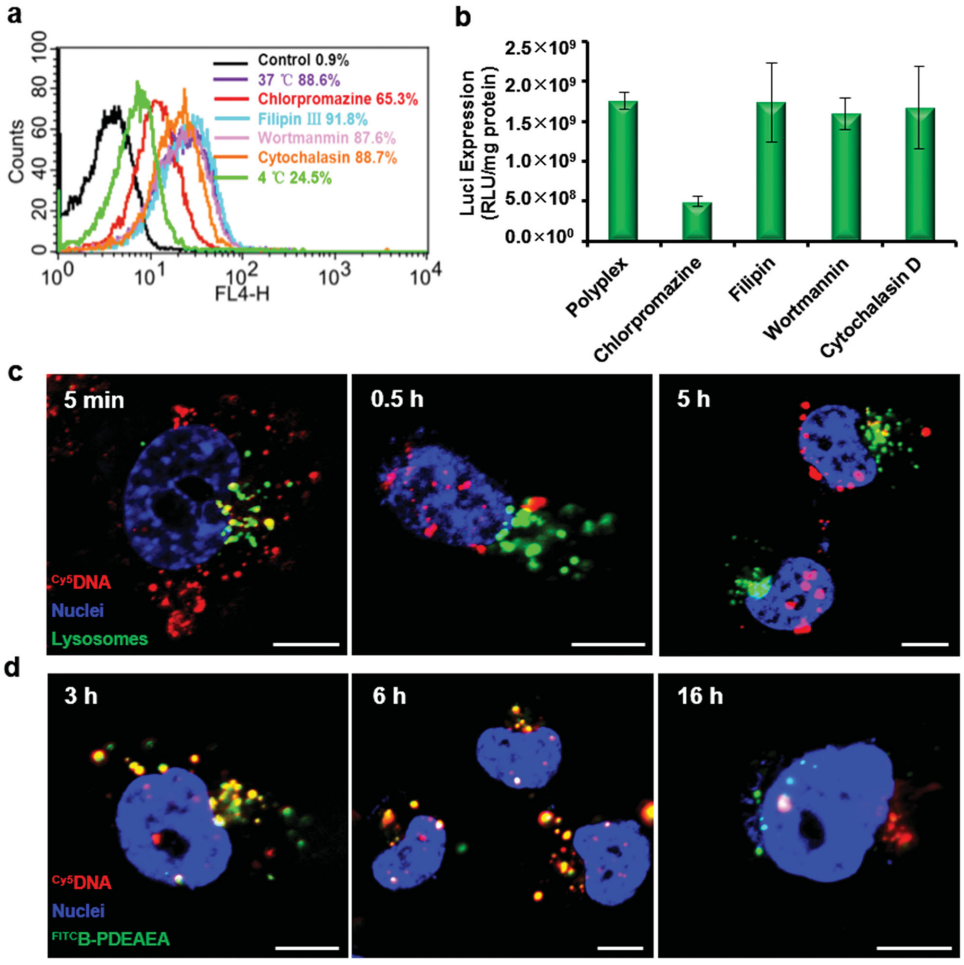

Figure 3. Cellular uptake and intracellular trafficking of B-PDEAEA/DNA polyplexes in A549 cells. a) Cy5-positive A549 cells measured by flow cytometry after treatment with polyplexes at 15 ng mL^{-1} ^{Cy5}DNA for 2 h in serum-free medium. The cells were cooled at 4 °C or separately pretreated with the inhibitors for 0.5 h at 37 °C. b) The luciferase gene transfection efficiency of polyplexes in A549 cells after 48 h. Cells were pretreated with each inhibitor for 0.5 h and then transfected at 2.2 μg mL^{-1} DNA for 4 h without serum and followed by 44 h culture. c) Confocal laser scanning microscopy images of A549 cells cultured with ^{Cy5}DNA polyplexes in serum-free medium at 0.64 μg mL^{-1} ^{Cy5}DNA for 5 min, 0.5 or 5 h (4 h followed by washing and then culturing in fresh medium for additional 1 h). ^{Cy5}DNA is shown in red, lysosomes dyed with LysoTracker Green are shown in green, and the cell nuclei stained with Hoechst 33342 are in blue. d) Observation of intracellular dissociation of ^{FITC}B-PDEAEA/^{Cy5}DNA polyplex of cells in serum-free medium at 0.64 μg mL^{-1} ^{Cy5}DNA at 3, 6, or 16 h (4 h followed by washing and then culturing in fresh medium for additional 2 or 12 h). ^{Cy5}DNA is shown in red, ^{FITC}B-PDEAEA is shown in green, and the cell nuclei stained with Hoechst 33342 are in blue. All scale bars are 10 μm.

(FITC)-labeled B-PDEAEA (^{FITC}B-PDEAEA). After the polyplexes were incubated with cells for 3 h, most green and red fluorescence was still overlapped and seen as yellow dots, while a few red dots were observed in the nuclei and some green dots were in the cytosol, which indicates some dissociation of the polyplexes. After incubation for 16 h, almost no yellow dots were observed in most cells, but separate red and green dots appeared (Figure 3d and see Figure S10 (Supporting Information) for the enlarged view of full images), confirming dissociation of the polyplexes triggered by intracellular ROS.

The intracellular fluorescence of ^{FITC}B-PDEAEA seemed faded away gradually, particularly after 12 h culturing (Figure S11a, Supporting Information), so the possible exocytosis of the polymer and the DNA was probed by dually labeled polyplexes. A549 cells were first cultured with ^{FITC}B-PDEAEA/^{Cy5}DNA polyplexes for 4 h and then the medium was replaced with fresh medium. The fluorescence intensity in the fresh medium of Cy5 did not change while the fluorescence intensity of FITC increased over time (Figure S11b,c, Supporting Information). These results indicate that after B-PDEAEA was oxidized by intracellular ROS and transformed into polyacrylic acid, it was removed from the cells by exocytosis, while the DNA remained in the cells, further confirming the dissociation of the polyplexes. This also suggests that unlike in siRNA delivery,[6a] endocytic recycling may not be a limiting factor in DNA delivery in this case.

For intravenous administration, the positive charges of the polyplexes must be shielded by coating the particles with polyethylene glycol (PEG)[24] or a lipid layer.[25] The boronic acid groups on the polyplex surface were first employed to coat the polyplexes with dopamine bisphenol-functionalized PEG (PEG-DA)[26] or hyaluronic acid (HA-DA).[27] Electrostatic adsorption was also used to coat the positively charged polyplexes with a negatively charged short peptide composed of

16 unit-polyglutamic acid (polyE), 6-unit neutral polyglycine, and an RGDK targeting sequence (arginine-glycine-aspartic acid-lysine, mRGD) (polyE–mRGD)[10] capable of binding to a αv-integrins and neuropilin-1 (Nrp-1), which are overexpressed on the endothelium of tumor vessels.[28] Coating PEG-DA, HA-DA, and polyE–mRGD to the polyplexes all produced very stable nanoparticles (Figure S12, Supporting Information). Some of them transfected cells well (Figure S13, Supporting Information) and were able to circulate long in the bloodstream, but unfortunately they did not induce sufficient luciferase expression in the tumor after intravenous administration (Figure S14, Supporting Information), very possibly due to the slower cellular internalization caused by the coating.

Motivated by our previous lipid-coated dendrimer nanoassembly[29] and multifunctional envelope-type nanodevice (MEND),[25] we hypothesized that while coating polyplexes with a PEGylated lipid layer would render them stealth properties, more importantly, the lipid layer might be engineered to fuse with the cell membrane and eject the polyplexes directly into the cytosol, mimicking the viropexis of a paramyxovirus, enabling the polyplexes to bypass the lysosomal pathway and thus avoid DNA degradation. Thus, a fusogenic lipid, 1,2-dioleoyl-*sn*-glycero-3-phosphoethanolamine (DOPE), and a PEGylated lipid 1,2-distearoyl-*sn*-glycero-3-phosphoethanolamine *N*-[methoxy(polyethylene glycol)-2000] (DSPE-PEG) were used as our previous report.[29] A negatively charged fusogenic lipid, cholesteryl hemisuccinate (CHEMS), was used as a helper lipid to bind the positively charged polyplex to make the surface hydrophobic for DOPE and DSPE-PEG coating. The lipid ratios were fine-tuned and found that at a DOPE/CHEMS/DSPE-PEG ratio of 7.65/2/1.35, where DSPE-PEG was 15% of total lipid, hydration of the polyplexes (*N*/*P* of 13) with the lipid film formed spherical FLPPs of around 120 nm in diameter with a zeta potential of −6 mV (**Figure 4**a and Figure S15a, Supporting Information). Upon addition of 0.24 vol% Triton X-100, the FLPP returned to the same size as the polyplexes, indicating that the lipid layer of the FLPP could be peeled off and each FLPP contained a single polyplex nanoparticle (Figure S15b, Supporting Information). In 10% serum medium, the PEGylated FLPPs expressed luciferase as efficiently as the noncoated polyplexes and was about ten times more efficient than the PEI polyplexes (Figure 4b). Significantly, the PEGylated FLPPs infected cells much more efficiently (42% cells) than the PEI polyplexes (5% cells) and noncoated B-PDEAEA polyplexes (*N*/*P* of 13) (9% cells) (Figure 4c and Figure S16, Supporting Information).

Cellular internalization of the FLPPs was subsequently probed by flow cytometry (Figure 4d). While low temperature suppressed cellular uptake of FLPPs, inhibitors including chlorpromazine, filipin III, wortmannin, and cytochalasin D did not affect cellular uptake of FLPPs (Figure 4d) and their luciferase expression (Figure 4e). These results indicate that cellular internalization of the FLPPs was not via common endocytosis, macropinocytosis, or phagocytosis. Cellular uptake of the FLPPs was confirmed in A549 cells by confocal microscopy. After the FLPPs with ^{Cy5}DNA (red) were incubated with cells for 1 h, the ^{Cy5}DNA was found attached to the cell membrane; after 6 h incubation, more red fluorescence was visible in the cytoplasm and nuclei (Figure 4f). Notably, at no time did the red fluorescence overlap with lysosomes (green) (Figure 4f and see Figure S17, Supporting Information, for the enlarged view of full images). These results may suggest that the FLPPs were internalized via membrane fusion and thus bypassed the endocytic pathway.

The fusion and intracellular dissociation of FLPPs were observed using the FLPPs triply labeled with ^{Cy5}DNA (red), ^{FITC}B-PDEAEA (green), and Rhodamine B-labeled DOPE (^{RhoB}DOPE, purple). After the FLPPs were incubated with cells for 1 h, the three colors were mainly found attached to the cell membrane and mostly overlapped. After 6 h incubation, the lipids were still on the cell membrane, some polymer and DNA (yellow spots) were colocalized in the cytoplasm, and most free DNA (red) was in cytoplasm, in the perinuclear region or in the nuclei. These results confirmed that the lipid layer fused with the cell membrane, releasing polyplexes into the cytoplasm and avoiding the endocytosis pathway; the polyplexes then dissociated in the cytoplasm as discussed above (Figure 4g and see Figure S18, Supporting Information, for the enlarged view of full images).

The lipid layer–cell membrane fusion process of the FLPPs was further tracked by fluorescence resonance energy transfer (FRET) technique as we reported.[29] DOPE lipids were separately labeled with a pair of FRET dyes, Rhodamine B and 7-nitro-2,1,3-benzoxadiazole (^{RhoB}DOPE and ^{NBD}DOPE), and the mixed lipid at a DOPE/^{RhoB}DOPE/^{NBD}DOPE molar ratio of 94:1:5 was used to fabricate the FRET FLPP (^{FRET}FLPP). If the lipid layer fuses with the cell membrane, the FRET emission at 585 nm excited at 450 nm will be inhibited. A FRET efficiency index, *R*, was calculated from the intensity ratio of ^{RhoB}DOPE fluorescence at 585 nm to ^{NBD}DOPE fluorescence at 525 nm when excited at 450 nm. The ^{FRET}FLPP solution had a strong FRET fluorescence peak with an *R* value of 3.8. The cells treated with ^{FRET}FLPP initially had the FRET peak with an *R* value of 1.3 at 3 h posttreatment, but the FRET peak gradually reduced and finally disappeared with an *R* value of only 0.6 after 48 h (Figure S19, Supporting Information).

Lipopolyplexes are generally taken up by cells via endocytosis,[30] for instance, the MEND developed by the Harashima group.[25a,31] The FLPPs developed here entered cells by fusion of their lipid envelope with the cell membrane, mimicking paramyxovirus. The membrane fusion rather than endocytosis of FLPPs was enabled by the right affinity of the lipid layer to the polyplexes. B-PDEAEA was a relatively hydrophobic polymer and adjusting the content of the anchoring lipid CHEMS in the lipid layer can fine tune the affinity. At the DOPE/CHEMS/DSPE-PEG ratio of 7.65/2/1.35, the FLPP's lipid layer was just sufficiently stable on the polyplexes surface but labile enough to leave from the polyplex surface once contacting the cell membrane.

The stealth property of the FLPPs was estimated by monitoring their blood clearance kinetics after intravenous injection. As shown in Figure S20 (Supporting Information), the blood clearance slowed as the DSPE-PEG content increased in the FLPPs. At 15% DSPE-PEG molar content relative to the total lipid, the FLPP clearance was very slow; 14% of the injected dose remained at 7 h postinjection (**Figure 5**a). The stability of FLPPs in the bloodstream was investigated using the FRET method. ^{FRET}FLPPs fabricated as described above had an *R*

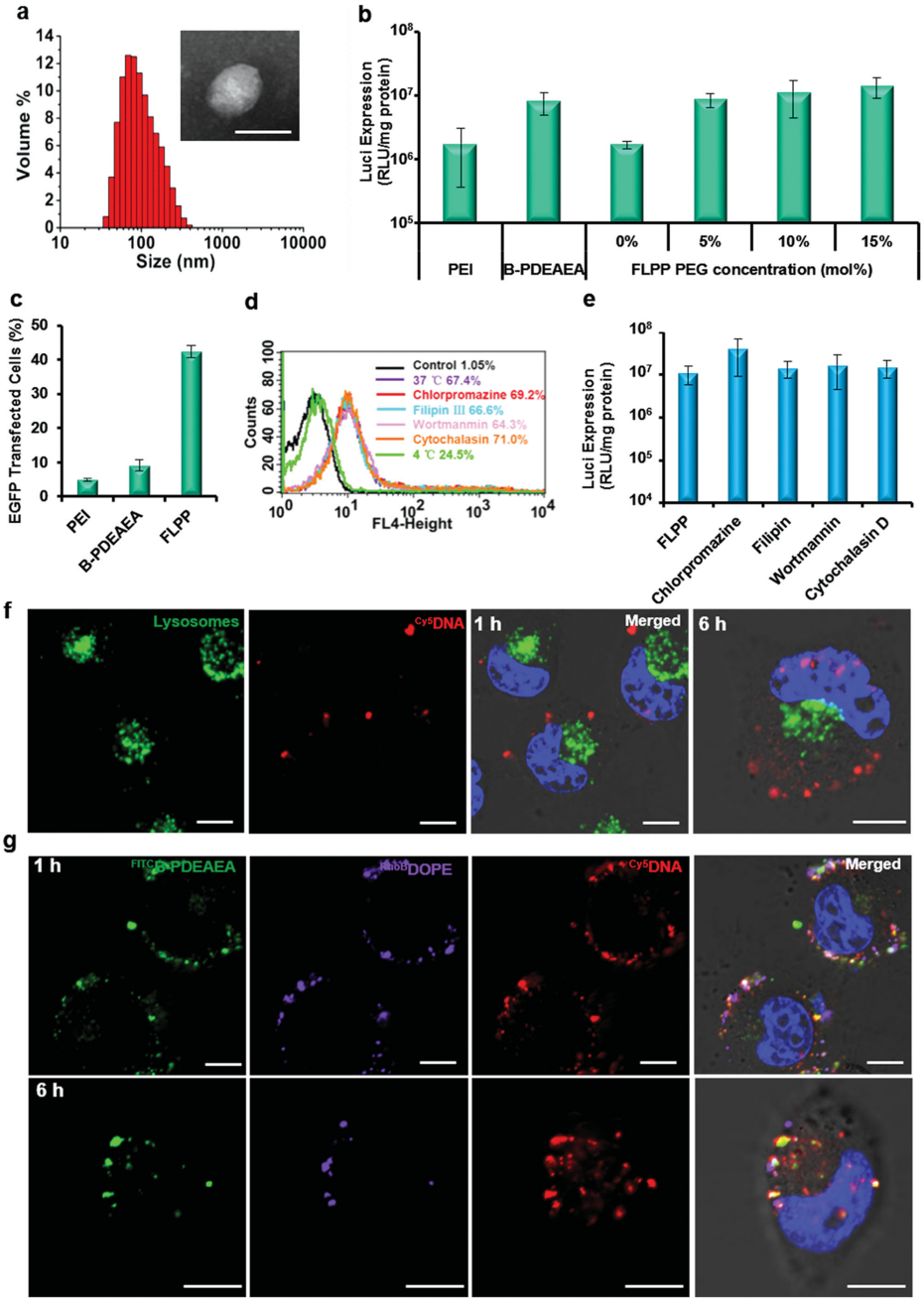

Figure 4. Characterization, gene expression, cellular uptake, and intracellular trafficking of FLPPs fabricated from B-PDEAEA polyplexes ($N/P = 13$). a) The size distribution measured by dynamic light scattering (DLS) and the morphology taken by transmission electron microscope (TEM) after stained with uranyl acetate of FLPPs with 15% DSPE-PEG. The scale bar is 100 nm. b) Luciferase gene transfection in 10% serum medium of the FLPPs containing different DSPE-PEG contents. A549 cells were cultured with FLPPs at 2.2 μg mL^{-1} DNA for 4 h in medium containing 10% serum followed by 44 h culture in fresh medium. c) EGFP gene transfection efficiency in A549 cells of FLPPs containing 15% DSPE-PEG in terms of GFP-positive cell percentage measured by flow cytometry compared with PEI polyplexes ($N/P = 7$); DNA dose at 4 μg mL^{-1}, 4 h transfection in 10% serum medium followed by 44 h culture in fresh medium. d) Cy5-positive A549 cells measured by flow cytometry after the cells were pretreated with each inhibitor for 0.5 h and then cultured with FLPPs (15% DSPE-PEG) at 15 ng mL^{-1} ^{Cy5}DNA in 10% serum medium for 2 h at 4 °C or at 37 °C. e) The effect of the inhibitor on the luciferase gene transfection efficiency of FLPPs (15% DSPE-PEG) in A549 cells. Cells were pretreated with each inhibitor for 0.5 h and then transfected at 2.2 μg mL^{-1} DNA in medium containing 10% serum for 4 h followed by 44 h culture in fresh medium. f) Confocal microscopy images of A549 cells cultured with ^{Cy5}DNA-FLPPs (15% DSPE-PEG) in 10% serum medium at 0.64 μg mL^{-1} ^{Cy5}DNA for 1 or 6 h (4 h followed by washing and then culturing in fresh medium for additional 2 h). ^{Cy5}DNA is shown in red; LysoTracker Green-dyed lysosomes are shown in green and cell nuclei stained with Hoechst 33342 are in blue. g) Observation of intracellular dissociation of triply labeled FLPPs (15% DSPE-PEG) with cells in 10% serum medium at 0.64 μg mL^{-1} ^{Cy5}DNA for 1 or 6 h (4 h followed by washing and then culturing in fresh medium for additional 2 h). ^{Cy5}DNA is shown in red, ^{FITC}B-PDEAEA is shown in green, ^{RhoB}DOPE is shown in purple, and cell nuclei stained with Hoechst 33342 are shown in blue. All scale bars are 10 μm.

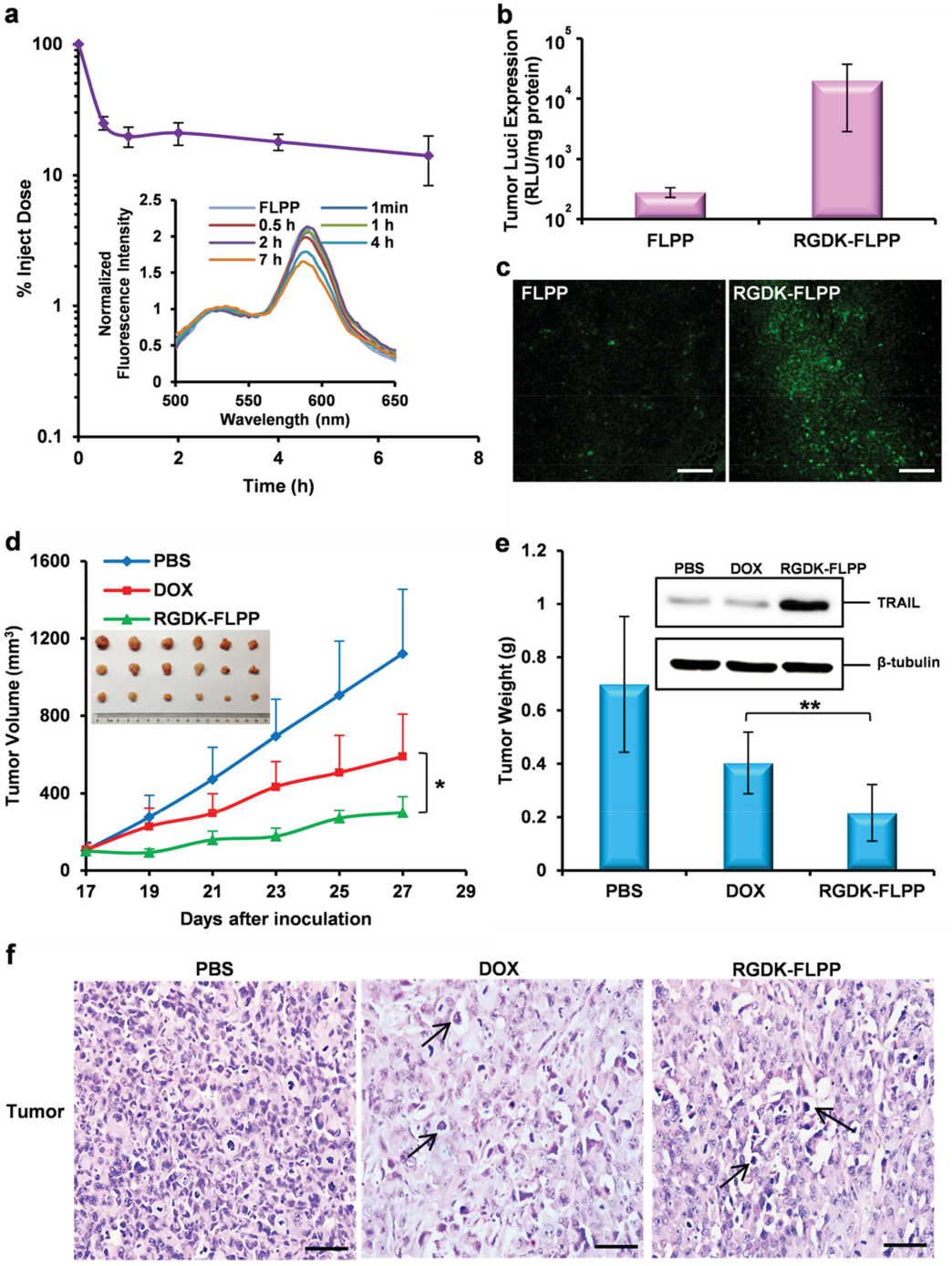

Figure 5. The blood clearance and stability, tumor gene expression, and anticancer activity of FLPPs ($N/P = 13$, 15% DSPE-PEG) loaded with TRAIL gene. a) The clearance kinetics from the blood circulation of FLPPs of Rhodamine B-labeled B-PDEAEA after administered via the tail vein; the inserted is the normalized FRET spectra excited at 450 nm of ^{FRET}FLPP in the blood plasma at timed intervals (the ^{FRET}FLPP contained 1% ^{RhoB}DOPE and 5% ^{NBD}DOPE of the total DOPE; $n = 3$, 15 μg DNA per mouse). b) Comparison between tumor luciferase expression of FLPPs with or without CRGDK at 48 h post i.v. injection. FLPPs were administered through tail vein injection ($n = 6$, 50 μg DNA per mouse) and c) their representative GFP fluorescence images of the tumor frozen sections; 10 μm thick. Scale bar = 200 μm. d) Antitumor activity of the TRAIL plasmid-loaded RGDK-FLPPs. A549 xenografted nude mice were treated intravenously with DOX (4 mg kg^{-1}), RGDK-FLPP (1 mg kg^{-1} TRAIL), or PBS ($n = 6$ each group) for five times at every 2 d when the tumor reached a size of ≈100 mm^3 (17 d after inoculation); each tumor was measured at the time of the injection. e) The averaged tumor weight and western blotting assay of TRAIL expression of each group at the end of the experiment on day 27 (* $P < 0.05$, ** $P < 0.01$). f) Representative histological features of tumors. Tissue paraffin sections were 5 μm thick. The sections were stained with hematoxylin–eosin and examined by light microscopy. Scale bar = 50 μm. Arrows show the nuclear shrinkage and fragmentation.

value of 2.1. After intravenous administration, the FLPPs in plasma had strong FRET signals at 585 nm and weak signals at 525 nm at different times even at 7 h postadministration with an *R* value of 1.7, indicating that the FLPPs were very stable in the blood circulation, explaining their slow blood clearance (Figure 5a, inset).

The tumor-homing peptide CRGDK[28] was coupled to DSPE-PEG (DSPE-PEG-RGDK, Figure S21, Supporting Information) to further enhance accumulation in tumors by active targeting. Indeed, the FLPP functionalized with 15% DSPE-PEG-RGDK (RGDK-FLPP) displayed tumor luciferase expression 71 times higher than the unmodified FLPP at 48 h postintravenous administration (Figure 5b), as also confirmed by much brighter GFP expression than in the tumors transfected by unmodified FLPPs and phosphate buffered saline (PBS) (Figure 5c and Figure S22, Supporting Information).

The in vivo therapeutic efficacy of RGDK-FLPPs was subsequently tested in subcutaneous A549 cell tumor-bearing mice using a therapeutic DNA, the TRAIL, which can preferentially induce apoptosis in malignant tumor cells, but not normal cells, and inhibit tumor-related angiogenesis.[32] The first-line anticancer drug DOX at a dose of 4 mg kg^{-1} was used as a positive control. Mice were intravenously treated with RGDK-FLPP/TRAIL at a TRAIL dose of 1 mg kg^{-1}. Both treatments with DOX and RGDK-FLPP/TRAIL led to significant inhibition of tumor growth compared to the PBS control, but the inhibitory effect of the RGDK-FLPP/TRAIL was higher than that of DOX ($P < 0.05$) (Figure 5d). After five treatments, the RGDK-FLPP/TRAIL had a 70% tumor inhibition rate in terms of tumor weight compared to 42% inhibition by DOX ($P < 0.01$) (Figure 5e). The therapeutic efficacy can be compared to the targeted delivery of the TRAIL gene to tumor xenografts by biodegradable poly(amine-co-esters) proposed by the Saltzman group.[10] Furthermore, treatment with DOX caused 14% weight loss but this was not seen in the RGDK-FLPP/TRAIL group (Figure S23, Supporting Information). Western blot analysis showed that TRAIL was strongly expressed in tumors treated by RGDK-FLPP/TRAIL (Figure 5e). Histological analysis by hematoxylin–eosin (H&E) staining (Figure 5f) showed that the tumors of the control group typically consisted of tightly packed cells, whereas extensive nuclear shrinkage and fragmentation (black arrow) was observed in the DOX and RGDK-FLPP/TRAIL groups, more obviously in the RGDK-FLPP/TRAIL-treated group. Histological analysis of heart tissues showed that the RGDK-FLPP/TRAIL-treated group had compact cardiomyocytes arranged in a clear structure similar to normal tissue, but those of the DOX treated group were characterized by myocardium tissue necrosis and disorganized myofibrillar arrays, typical of cardiomyocyte damage induced by DOX (Figure S24, Supporting Information).[33]

We have demonstrated a charge-reversal polymer B-PDEAEA which is strongly positively charged and effectively packages DNA into nanoparticles but becomes negatively charged once triggered by intracellular ROS. The resulting ROS-responsive polyplexes show higher gene transfection efficiency than the traditional gold standard. The polyplexes are coated with a fusogenic lipid layer to form CRGKD-targeting PEGylated virus-mimicking fusogenic lipopolyplexes (FLPPs), which are stable and long-circulating in vivo and achieve significantly enhanced gene expression in tumor and anticancer therapeutic activity, even more effectively than the potent anticancer drug DOX. The novel vector is capable of mimicking viropexis, thus avoiding endosomal DNA degradation and not interfering with DNA transcription. Its in vivo tumor targeting ability and high gene expression merit it for further study of gene therapy.

Supporting Information

Supporting Information is available from the Wiley Online Library or from the author.

Acknowledgements

X.L. and J.X. contributed equally to this work. The authors thank the National Basic Research Program (2014CB931900), the National Natural Science Foundation Key Program (51390481), and the National Fund for Distinguished Young Scholars (50888001) for financial supports. All animal studies were approved by the Animal Care and Use Committee of Zhejiang University in accordance with the guidelines for the care and use of laboratory animals.

Received: September 1, 2015
Revised: October 28, 2015
Published online: December 14, 2015

[1] a) L. Naldini, U. Blomer, P. Gallay, D. Ory, R. Mulligan, F. H. Gage, I. M. Verma, D. Trono, *Science* **1996**, *272*, 263; b) H. Farmer, N. McCabe, C. J. Lord, A. N. J. Tutt, D. A. Johnson, T. B. Richardson, M. Santarosa, K. J. Dillon, I. Hickson, C. Knights, N. M. B. Martin, S. P. Jackson, G. C. M. Smith, A. Ashworth, *Nature* **2005**, *434*, 917; c) H. Yin, R. L. Kanasty, A. A. Eltoukhy, A. J. Vegas, J. R. Dorkin, D. G. Anderson, *Nat. Rev. Genet.* **2014**, *15*, 541; d) C. J. Cheng, R. Bahal, I. A. Babar, Z. Pincus, F. Barrera, C. Liu, A. Svoronos, D. T. Braddock, P. M. Glazer, D. M. Engelman, W. M. Saltzman, F. J. Slack, *Nature* **2015**, *518*, 107; e) C. Sheridan, *Nat. Biotechnol.* **2015**, *33*, 569.

[2] a) M. A. Mintzer, E. E. Simanek, *Chem. Rev.* **2009**, *109*, 259; b) R. Kanasty, J. R. Dorkin, A. Vegas, D. Anderson, *Nat. Mater.* **2013**, *12*, 967; c) J. E. Dahlman, C. Barnes, O. F. Khan, A. Thiriot, S. Jhunjunwala, T. E. Shaw, Y. P. Xing, H. B. Sager, G. Sahay, L. Speciner, A. Bader, R. L. Bogorad, H. Yin, T. Racie, Y. Z. Dong, S. Jiang, D. Seedorf, A. Dave, K. S. Sandhu, M. J. Webber, T. Novobrantseva, V. M. Ruda, A. K. R. Lytton-Jean, C. G. Levins, B. Kalish, D. K. Mudge, M. Perez, L. Abezgauz, P. Dutta, L. Smith, K. Charisse, M. W. Kieran, K. Fitzgerald, M. Nahrendorf, D. Danino, R. M. Tuder, U. H. von Andrian, A. Akinc, D. Panigrahy, A. Schroeder, V. Koteliansky, R. Langer, D. G. Anderson, *Nat. Nanotechnol.* **2014**, *9*, 648.

[3] a) A. Akinc, D. M. Lynn, D. G. Anderson, R. Langer, *J. Am. Chem. Soc.* **2003**, *125*, 5316; b) J. J. Green, R. Langer, D. G. Anderson, *Acc. Chem. Res.* **2008**, *41*, 749; c) Y. Z. Dong, A. A. Eltoukhy, C. A. Alabi, O. F. Khan, O. Veiseh, J. R. Dorkin, S. Sirirungruang, H. Yin, B. C. Tang, J. M. Pelet, D. L. Chen, Z. Gu, Y. Xue, R. Langer, D. G. Anderson, *Adv. Healthcare Mater.* **2014**, *3*, 1392; d) K. A. Whitehead, J. R. Dorkin, A. J. Vegas, P. H. Chang, O. Veiseh, J. Matthews, O. S. Fenton, Y. L. Zhang, K. T. Olejnik, V. Yesilyurt, D. L. Chen, S. Barros, B. Klebanov, T. Novobrantseva, R. Langer, D. G. Anderson, *Nat. Commun.* **2014**, *5*, 4277.

[4] a) P. Xu, S. Li, Q. Li, E. A. Van Kirk, J. Ren, W. J. Murdoch, Z. Zhang, M. Radosz, Y. Shen, *Angew. Chem. Int. Ed.* **2008**, *47*, 1260;

b) H. Y. Kuchelmeister, S. Karczewski, A. Gutschmidt, S. Knauer, C. Schmuck, *Angew. Chem. Int. Ed.* **2013**, *52*, 14016; c) M. M. Wang, H. M. Liu, L. Li, Y. Y. Cheng, *Nat. Commun.* **2014**, *5*, 3053.

[5] a) P. S. Xu, G. K. Quick, Y. Yeo, *Biomaterials* **2009**, *30*, 5834; b) C. Xu, M. Sui, J. Tang, Y. Shen, *Chin. J. Polym. Sci.* **2011**, *29*, 274; c) Y. He, Y. Nie, G. Cheng, L. Xie, Y. Shen, Z. Gu, *Adv. Mater.* **2014**, *26*, 1534; d) Y. Li, H. Tian, J. Ding, L. Lin, J. Chen, S. Gao, X. S. Chen, *Adv. Healthcare Mater.* **2015**, *4*, 1369; e) H. Z. Jia, W. Zhang, X. L. Wang, B. Yang, W. H. Chen, S. Chen, G. Chen, Y. F. Zhao, R. X. Zhuo, J. Feng, X. Z. Zhang, *Biomater. Sci.* **2015**, *3*, 1066.

[6] a) G. Sahay, W. Querbes, C. Alabi, A. Eltoukhy, S. Sarkar, C. Zurenko, E. Karagiannis, K. Love, D. Chen, R. Zoncu, Y. Buganim, A. Schroeder, R. Langer, D. G. Anderson, *Nat. Biotechnol.* **2013**, *31*, 653; b) Z. U. Rehman, D. Hoekstra, I. S. Zuhorn, *ACS Nano* **2013**, *7*, 3767.

[7] a) R. Weissleder, K. Kelly, E. Y. Sun, T. Shtatland, L. Josephson, *Nat. Biotechnol.* **2005**, *23*, 1418; b) J. J. Green, E. Chiu, E. S. Leshchiner, J. Shi, R. Langer, D. G. Anderson, *Nano Lett.* **2007**, *7*, 874; c) J. G. Li, X. S. Yu, Y. Wang, Y. Y. Yuan, H. Xiao, D. Cheng, X. T. Shuai, *Adv. Mater.* **2014**, *26*, 8217; d) H. Ragelle, S. Colombo, V. Pourcelle, K. Vanvarenberg, G. Vandermeulen, C. Bouzin, J. Marchand-Brynaert, O. Feron, C. Foged, V. Preat, *J. Controlled Release* **2015**, *211*, 1; e) J. Conde, C. C. Bao, Y. Q. Tan, D. X. Cui, E. R. Edelman, H. S. Azevedo, H. J. Byrne, N. Artzi, F. R. Tian, *Adv. Funct. Mater.* **2015**, *25*, 4183.

[8] a) J. Zabner, A. J. Fasbender, T. Moninger, K. A. Poellinger, M. J. Welsh, *J. Biol. Chem.* **1995**, *270*, 18997; b) H. Pollard, J. S. Remy, G. Loussouarn, S. Demolombe, J. P. Behr, D. Escande, *J. Biol. Chem.* **1998**, *273*, 7507.

[9] a) G. Byk, B. Wetzer, M. Frederic, C. Dubertret, B. Pitard, G. Jaslin, D. Scherman, *J. Med. Chem.* **2000**, *43*, 4377; b) R. A. Jones, C. Y. Cheung, F. E. Black, J. K. Zia, P. S. Stayton, A. S. Hoffman, M. R. Wilson, *Biochem. J.* **2003**, *372*, 65; c) M. Bikram, C. H. Ahn, S. Y. Chae, M. Y. Lee, J. W. Yockman, S. W. Kim, *Macromolecules* **2004**, *37*, 1903; d) H. Lomas, I. Canton, S. MacNeil, J. Du, S. P. Armes, A. J. Ryan, A. L. Lewis, G. Battaglia, *Adv. Mater.* **2007**, *19*, 4238; e) X. A. Jiang, Y. R. Zheng, H. H. Chen, K. W. Leong, T. H. Wang, H. Q. Mao, *Adv. Mater.* **2010**, *22*, 2556; f) X. X. Zhang, C. A. H. Prata, J. A. Berlin, T. J. McIntosh, P. Barthelemy, M. W. Grinstaff, *Bioconjugate Chem.* **2011**, *22*, 690; g) S. J. Tseng, Z. X. Liao, S. H. Kao, Y. F. Zeng, K. Y. Huang, H. J. Li, C. L. Yang, Y. F. Deng, C. F. Huang, S. C. Yang, P. C. Yang, I. M. Kempson, *Nat. Commun.* **2015**, *6*, 6456; h) S. J. Park, W. Park, K. Na, *Adv. Funct. Mater.* **2015**, *25*, 3472.

[10] J. Zhou, J. Liu, C. J. Cheng, T. R. Patel, C. E. Weller, J. M. Piepmeier, Z. Jiang, W. M. Saltzman, *Nat. Mater.* **2012**, *11*, 82.

[11] A. Gopin, N. Pessah, M. Shamis, C. Rader, D. Shabat, *Angew. Chem. Int. Ed.* **2003**, *42*, 327.

[12] a) M. T. Epperson, C. E. Hadden, T. G. Waddell, *J. Org. Chem.* **1995**, *60*, 8113; b) N. P. Truong, W. Y. Gu, I. Prasadam, Z. F. Jia, R. Crawford, Y. Xiao, M. J. Monteiro, *Nat. Commun.* **2013**, *4*, 1902; c) P. Cotanda, D. B. Wright, M. Tyler, R. K. O'Reilly, *J. Polym. Sci. Polym. Chem.* **2013**, *51*, 3333.

[13] a) D. Trachootham, J. Alexandre, P. Huang, *Nat. Rev. Drug Discov.* **2009**, *8*, 579; b) Y. Kuang, K. Balakrishnan, V. Gandhi, X. Peng, *J. Am. Chem. Soc.* **2011**, *133*, 19278.

[14] a) K. E. Broaders, S. Grandhe, J. M. Frechet, *J. Am. Chem. Soc.* **2011**, *133*, 756; b) C. C. Song, R. Ji, F. S. Du, Z. C. Li, *Macromolecules* **2013**, *46*, 8416.

[15] a) E. W. Miller, A. E. Albers, A. Pralle, E. Y. Isacoff, C. J. Chang, *J. Am. Chem. Soc.* **2005**, *127*, 16652; b) B. C. Dickinson, C. J. Chang, *J. Am. Chem. Soc.* **2008**, *130*, 9638; c) D. Srikun, E. W. Miller, D. W. Domaille, C. J. Chang, *J. Am. Chem. Soc.* **2008**, *130*, 4596; d) X. Sun, Q. Xu, G. Kim, S. E. Flower, J. P. Lowe, J. Yoon, J. S. Fossey, X. Qian, S. D. Bull, T. D. James, *Chem. Sci.* **2014**, *5*, 3368.

[16] a) A. Matsumoto, N. Sato, K. Kataoka, Y. Miyahara, *J. Am. Chem. Soc.* **2009**, *131*, 12022; b) A. Matsumoto, H. Cabral, N. Sato, K. Kataoka, Y. Miyahara, *Angew. Chem. Int. Ed.* **2010**, *49*, 5494; c) S. Deshayes, H. Cabral, T. Ishii, Y. Miura, S. Kobayashi, T. Yamashita, A. Matsumoto, Y. Miyahara, N. Nishiyama, K. Kataoka, *J. Am. Chem. Soc.* **2013**, *135*, 15501.

[17] a) M. Piest, J. F. Engbersen, *J. Controlled Release* **2011**, *155*, 331; b) M. Naito, T. Ishii, A. Matsumoto, K. Miyata, Y. Miyahara, K. Kataoka, *Angew. Chem. Int. Ed.* **2012**, *51*, 10751.

[18] a) J. Wang, W. Wu, Y. Zhang, X. Wang, H. Qian, B. Liu, X. Jiang, *Biomaterials* **2014**, *35*, 866; b) J. Y. Lee, S. J. Chung, H. J. Cho, D. D. Kim, *Adv. Funct. Mater.* **2015**, *25*, 3705.

[19] a) S. G. Peisajovich, Y. Shai, *Biochim. Biophys. Acta* **2003**, *1614*, 122; b) S. A. Connolly, R. A. Lamb, *Virology* **2006**, *355*, 203.

[20] C. Arigita, N. J. Zuidam, D. J. Crommelin, W. E. Hennink, *Pharm. Res.* **1999**, *16*, 1534.

[21] a) Y. Li, M. A. Trush, *Biochem. Biophys. Res. Commun.* **1998**, *253*, 295; b) W. Yan, W. Chen, L. Huang, *J. Controlled Release* **2008**, *130*, 22.

[22] M. Piest, M. Ankone, J. F. J. Engbersen, *J. Controlled Release* **2013**, *169*, 266.

[23] N. Murthy, J. R. Robichaud, D. A. Tirrell, P. S. Stayton, A. S. Hoffman, *J. Controlled Release* **1999**, *61*, 137.

[24] a) H. Otsuka, Y. Nagasaki, K. Kataoka, *Adv. Drug Deliv. Rev.* **2003**, *55*, 403; b) B. Romberg, W. E. Hennink, G. Storm, *Pharm. Res.* **2008**, *25*, 55; c) F. M. Kievit, O. Veiseh, N. Bhattarai, C. Fang, J. W. Gunn, D. Lee, R. G. Ellenbogen, J. M. Olson, M. Q. Zhang, *Adv. Funct. Mater.* **2009**, *19*, 2244; d) S. Essex, G. Navarro, P. Sabhachandani, A. Chordia, M. Trivedi, S. Movassaghian, V. P. Torchilin, *Gene Ther.* **2015**, *22*, 257.

[25] a) K. Kogure, R. Moriguchi, K. Sasaki, M. Ueno, S. Futaki, H. Harashima, *J. Controlled Release* **2004**, *98*, 317; b) H. Hatakeyama, H. Akita, H. Harashima, *Adv. Drug Deliv. Rev.* **2011**, *63*, 152.

[26] J. Xie, C. Xu, N. Kohler, Y. Hou, S. Sun, *Adv. Mater.* **2007**, *19*, 3163.

[27] X. M. Zhang, Z. Y. Li, X. B. Yuan, Z. D. Cui, X. J. Yang, *Appl. Surf. Sci.* **2013**, *284*, 732.

[28] a) K. N. Sugahara, T. Teesalu, P. P. Karmali, V. R. Kotamraju, L. Agemy, O. M. Girard, D. Hanahan, R. F. Mattrey, E. Ruoslahti, *Cancer Cell* **2009**, *16*, 510; b) K. N. Sugahara, T. Teesalu, P. P. Karmali, V. R. Kotamraju, L. Agemy, D. R. Greenwald, E. Ruoslahti, *Science* **2010**, *328*, 1031; c) T. Wei, J. Liu, H. Ma, Q. Cheng, Y. Huang, J. Zhao, S. Huo, X. Xue, Z. Liang, X. J. Liang, *Nano Lett.* **2013**, *13*, 2528.

[29] Q. Sun, X. Sun, X. Ma, Z. Zhou, E. Jin, B. Zhang, Y. Shen, E. A. Van Kirk, W. J. Murdoch, J. R. Lott, T. P. Lodge, M. Radosz, Y. Zhao, *Adv. Mater.* **2014**, *26*, 7615.

[30] a) E. S. Scott, J. W. Wiseman, M. J. Evans, W. H. Colledge, *J. Gene Med.* **2001**, *3*, 125; b) M. F. M. Mustapa, S. M. Grosse, L. Kudsiova, M. Elbs, E. A. Raiber, J. B. Wong, A. P. R. Brain, H. E. J. Armer, A. Warley, M. Keppler, T. Ng, M. J. Lawrence, S. L. Hart, H. C. Hailes, A. B. Tabor, *Bioconjugate Chem.* **2009**, *20*, 518; c) Y. Nie, M. Gunther, Z. W. Gu, E. Wagner, *Biomaterials* **2011**, *32*, 858.

[31] H. Akita, A. Kudo, A. Minoura, M. Yamaguti, I. A. Khalil, R. Moriguchi, T. Masuda, R. Danev, K. Nagayama, K. Kogure, H. Harashima, *Biomaterials* **2009**, *30*, 2940.

[32] a) S. Kagawa, C. He, J. Gu, P. Koch, S. J. Rha, J. A. Roth, S. A. Curley, L. C. Stephens, B. L. Fang, *Cancer Res.* **2001**, *61*, 3330; b) H. Matsubara, Y. Mizutani, F. Hongo, H. Nakanishi, Y. Kimura, S. Ushijima, A. Kawauchi, T. Tamura, T. Sakata, T. Miki, *Mol. Cancer Ther.* **2006**, *5*, 2165.

[33] E. Jin, B. Zhang, X. Sun, Z. Zhou, X. Ma, Q. Sun, J. Tang, Y. Shen, E. Van Kirk, W. J. Murdoch, M. Radosz, *J. Am. Chem. Soc.* **2013**, *135*, 933.